THE SUPER-THERMOHYDROPHOBIC EFFECT

J.M.Floryan[a)]*M.Z.Hossain & D.Floryan*
Department of Mechanical and Materials Engineering
The University of Western Ontario
London, Ontario, N6A 5B9, Canada

Summary: Drag associated with flow of liquids can be reduced by the so-called Super-Hydrophobic effect [1]. This effect results from a combination of the hydrophobicity of the liquid and surface material, and surface topography. When a Super-Hydrophobic surface is submerged inside a liquid, gas bubbles get trapped in surface micro-pores effectively reducing shear stress experienced by the liquid, as shear between the liquid and the solid is replaced by shear between the liquid and the gas. Here we show that a similar effect can be produced by spatially distributed heating which leads to formation of buoyancy-driven separation bubbles. We refer to this phenomenon as the Super-ThermoHydrophobic Effect.

INTRODUCTION

The available knowledge about the Super-Hydrophobic effect relates to motion of water with bubbles of air forming in surface pores and originates in the unique water-repellent properties of the lotus leaf [2]. The drag reducing abilities can be increased by correct shaping of surface pores/roughness[3] and by increasing hydrophobicity through changes in surface chemistry [4-8]. The laminar drag reduction has been demonstrated both theoretically and experimentally in the case of laminar [9-13] as well as turbulent [14-15] flows. Presence of two phases is essential for the drag reduction as shear between liquid and solid gets replaced by shear between liquid and gas. The purpose of this work is to demonstrate the existence of a Super-Hydrophobic-like effect which provides a meaningful drag reduction in single phase fluids. This effect is created by use of a pattern of localized heating-cooling that leads to the formation of separation bubbles that isolate the main stream from the direct contact with the bounding walls and in this way reduces shear. The Super-ThermoHydrophobic Effect, remains effective for very small Reynolds numbers as stronger flows wash separation bubbles away. It is of interest for applications in nano- and micro-channels where system performance suffers from limitations associated with large pressure losses. The presented results are for the Prandtl number Pr=0.71 (air) to demonstrate the level of drag reduction that can be achieved in gases.

MODEL PROBLEM

Consider steady flow of fluid confined in a channel bounded by two parallel walls extending to $\pm\infty$ in the x-direction and placed at a distance 2h apart from each other with the gravitational acceleration g acting in the negative y-direction. The flow is driven in the positive x-direction by a pressure gradient with a maximum velocity U_{max}. The fluid is incompressible and Newtonian with thermal conductivity k, specific heat c, thermal diffusivity $\kappa=k/\rho c$, kinematic viscosity ν, dynamic viscosity μ, thermal expansion coefficient Γ and variations of the density ρ that follow the Boussinesq approximation. The lower wall is subject to a periodic heating resulting in wall temperatures in the form $\theta_L(x)=\cos(\alpha x)/2$, $\theta_U(x)=0$, where θ denotes the relative temperature scaled with the amplitude of the peak to peak temperature variations along the wall T_d, i.e., $\theta=(T-T_U)/T_d$, T denotes the absolute temperature, $\lambda=2\pi/\alpha$ is the wavelength of the heating, subscripts L and U refer to the lower and upper walls, respectively, and the half channel height h has been used as the length scale. The intensity of the heating is measured in terms of the Rayleigh number defined as $Ra_p=g\Gamma h^3 T_d/\nu\kappa$. The problem of determination of potential drag reduction is posed as a problem of finding additional pressure gradient that is required to drive the same mass flux through the heated as well as through an isothermal channel. In order to determine this pressure drop, the flow and temperature fields are represented as $\mathbf{u}(x,y)=[\mathrm{Re}\,u_0(y)+u_1(x,y), v_1(x,y)]$, $\theta(x,y)=\mathrm{Pr}^{-1}\theta_0(x,y)+\theta_1(x,y)$, $p(x,y)=\mathrm{Re}^2 p_0(x)+p_1(x,y)$, where $u_0(y)=1-y^2$, $p_0(x)=-2x/\mathrm{Re}$ have been scaled with U_{max} and ρU_{max}^2, respectively, $\mathrm{Re}=U_{max}h/\nu$ is the Reynolds number, $\mathbf{u}$ has been scaled with $U_v=\nu/h$ where $U_{max}/U_v=\mathrm{Re}$, p and p_1 have been scaled with ρU_v^2, θ and θ_1 have been scaled with $T_v=T_d\nu/\kappa$ where $\mathrm{Pr}=\nu/\kappa$ is the Prandtl number, and $\theta_0(x,y)=[-\sinh(\alpha y)/\sinh(\alpha)+\cosh(\alpha y)/\cosh(\alpha)]\cos(\alpha x)/4$ is the conductive temperature field. The field equations consist of the continuity, Navier-Stokes and energy equations subject to homogeneous boundary conditions. The mean pressure gradient has the form $\partial p/\partial x|_{mean}=\mathrm{Re}\,(-2+A/\mathrm{Re})$ where positive A identifies drag reduction.

DISCUSSION

Various flow topologies results from the formation of separation bubbles at the lower and upper walls as well as in the flow interior (see Fig.1); in total six combinations are possible. Increase of Re reduces their size and eventually washes them away (see Fig.2). Increase Ra_p extends the range of Re where the bubbles can survive. Presence of bubbles affects

[a)]Corresponding author. Email: mfloryan@eng.uwo.ca

direction and magnitude of shear and thus changes the required pressure drop. The largest drag reduction is associated with bubbles present at both walls and is independent of Re for Re<1 (see Fig.3); increase of flow intensity beyond Re>1 quickly eliminates this effect. The drag reduction is remarkable when one takes into account the contorted path that fluid elements must follow with significant increase in the mean length of the path and significant reduction of the cross-sectional flow area compared with the unheated case. The reduction strongly depends on the heating wave number with the largest drop occurring for α=0(1) (see Fig.3). It increases proportionally to Ra_p^2 until a saturation develops due to formation of the in-flow bubbles and rise in the associated shear (see Fig.4). Drag reduction reaches A/Re $\approx$ 0.84 (42% of the isothermal value) for Ra_p=2000 and A/Re $\approx$ 1.74 (87%) for Ra_p=5000.

Variability of the flow separation with Ra_p and Re can be utilized in developing various flow control strategies. Flow rate can be controlled by increasing/decreasing heating level while keeping the overall pressure drop the same. A fraction of fluid volume can be trapped inside separation bubbles for a specified length of time and then removed from the conduit by increasing Re; slowing down the flow would re-create bubbles but with different fluid elements trapped inside. Combination of heating and flow strength provides tool for management of chemical reactions in micro-vessels, e.g., polymerase chain reaction amplification of DNA [16]. The effectiveness of the process can be increased by combining heating with proper surface topography.

CONCLUSIONS

It is demonstrated that a pattern of heating applied to a horizontal channel results in a significant drag reduction. This effect occurs due to the formation of separation bubbles which isolate the flowing stream from the bounding solid walls and thus reduce shear acting on the stream.

References

[1] Rothstein, J.P., 2010, Slip on superhydrophobic surfaces, *Annu. Rev. Fluid Mech.* **42**, 89-109.

[2] Barthlott, W., Neinhuis, C., 1977, Purity of sacred lotus, or escape from contamination in biological surfaces, *Planta* **202**, 1-8.

[3] Samaha, M.A., Tafreshi, H.V., Gad-el-Hak, 2011, Modeling drag reduction and meniscus stability of superhydrophobic surfaces comprised of random roughness, *Phys. Fluids* **23**, 012001.

[4] Gao, L., McCarthy, T.J., 2006, A perfectly hydrophobic surface (θ(A)/θ(R)=180°/180°), *J. Am. Chem.Soc.* **128**, 9052-9053.

[5] Quéré, D., 2008, Wetting and roughness, *Annu. Rev. Mater. Res*. **38**, 71-99.

[6] Reyssat, M., Yeomans, J.M., Quéré, D., 2008, Impalement of fakir drops, *Europhys. Lett.* **81**, 26006.

[7] Xi, Z., Feng, S., Jia, N., Yugui, J., Zhiqiang, W., 2008, Superhydrophobic surfaces: from structural control to functional application, *J.Material Chemistry* **18**, 621-633.

[8] Zhou, M., Li, J., Wu C., Zhou, X., Cai, L., 2011, Fluid drag reduction on superhydrophobic surfaces coated with carbon nanotube forest (CNTs), *Soft Matter* **7**, 4391-4396.

[9] Ou, J., Perot, J.B., Rothstein, J.P., 2004, Laminar drag reduction in microchannels using ultrahydrophobic surfaces, *Phys. Fluids* **16**, 4635.

[10] Ou, J., Rothstein, J.P., 2005, Direct velocity measurements of the flow past drag-reducing ultrahydrophobic surfaces, *Phys. Fluids* **17**, 103606.

[11] Joseph, P., Cottin-Bizonne, C., Benoit, J.M., Ybert, C., Journet, C., Tabeling, P., Bocquet, L., 2006, Slippage of water past superhydrophobic carbon nanotube forests in microchannels, *Phys. Rev. Lett*. **97**, 156104.

[12] Truesdell, R., Mammoli, P., Vorobieff, P., van Swol, P., Brinker, C.J., 2006, Drag reduction on a patterned superhydrophobic surface, *Phys. Rev. Lett*. **97**, 044504.

[13] Teo, C.J., Khoo, B.C., 2009, Analysis of Stokes flow in microchannels with superhydrophobic surfaces containing a periodic array of micro-grooves, *Microfluid. Nanofluid* 7, 353.

[14] Martell, M., Perot, J.B., Rothstein, J.P., 2009, Direct numerical simulations of turbulent flows over superhydrophobic surfaces, *J. Fluid Mech*. **620**, 31-41.

[15] Daniello, R., Waterhouse, N.E., Rothstein, J.P., 2009, Turbulent drag reduction using superhydrophobic surfaces, *Phys. Fluids* **21**, 085103.

[16] Krishnan, M., Ugaz, V.M., Burns, M.A., 2002, PCR in a Rayleigh-Bénard Convection Cell, *Science* **298**, 793.

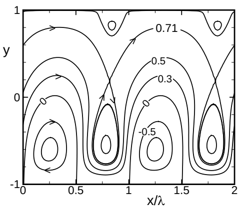

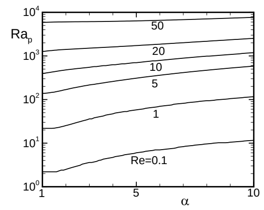

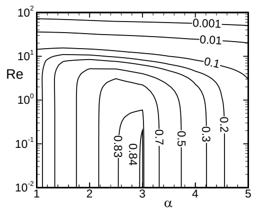

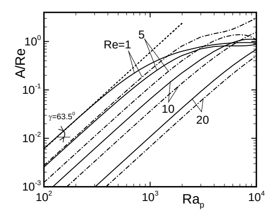

Figure 1. Flow pattern for Re = 1, α = 5, Ra_p = 5000.	Figure 2. Conditions required for formation of separation bubbles at the lower wall.	Figure 3. Variations of A/Re as a function of α and Re for Ra_p=2000.	Figure 4. Variations of A/Re as a function of Ra_p and Re for α=2 (solid lines) and α=3 (dash-dot lines).